Journal of Superconductivity and Novel Magnetism (2023) 36:931–938
https://doi.org/10.1007/s10948-023-06529-0

ORIGINAL PAPER

Magnetocaloric Effect in R_6Fe_{23}: R = Dy, Ho, Er, and Tm

Raghda Abu Elnasr[1] · Samy H. Aly[1] · Sherif Yehia[2] · Fatema Z. Mohammad[1]

Received: 10 December 2022 / Accepted: 12 February 2023 / Published online: 1 March 2023

Abstract
We present a mean field study on the R_6Fe_{23} system, where R = Dy, Ho, Er, and Tm, to calculate the magnetization, magnetic heat capacity, and the magnetocaloric effect (MCE) (isothermal entropy change (ΔS_m) and the adiabatic temperature change (ΔT_{ad})) for different field changes up to 5 T and at temperatures ranging from 0 to 600 K. The maximum ΔS_m, using the trapezoidal method, for the R_6Fe_{23} system is in the range 4.9–9.8 J/K mol, and the maximum ΔT_{ad} is in the range 9.56–15.17 K for a field change $\Delta H = 5$ T. The largest ΔS_m and largest ΔT_{ad} are found for Tm_6Fe_{23} to be 9.8 J/K mol and 15.17 K at Curie temperature $T_c = 489$ K, for $\Delta H = 5$ T. The relative cooling power RCP(S) is in the range 148–560 J/mol for $\Delta H = 5$ T, which is comparable to that of bench-mark materials, e.g., Gd. Also, the RCP based on the adiabatic temperature change, RCP(T) is in the range 449–1092 K^2 for $\Delta H = 5$ T, which is comparable also to that of bench-mark materials, e.g., Gd. We investigated the type of phase transition in the light of universal curves, Arrott plots, and the behavior of the magnetic moment, magnetic heat capacity, and MCE (ΔS_m, ΔT_{ad}), which confirm that the type of phase transition at T_c of this system is second-order phase transition (SOPT). A calculation of some critical exponents adds more evidence that the MFT is fairly suitable to handle the aforementioned properties in the studied systems.

Keywords Magnetocaloric effect (MCE) · Mean field theory (MFT) · Critical exponents

1 Introduction

The magnetocaloric effect (MCE) has been discussed before for magnetic and rare-earth intermetallic compounds [1–3]. There are different functional materials useful for technological applications such as magnetic refrigeration technology, which is hoped to be environmentally safer and a more efficient alternative to traditional refrigeration technology [4–6]. Many studies, on MCE, were done by using the mean field theory MFT, e.g., $TmFe_2$ [7], $R_2Fe_{14}B$ [8], Gd-Co [9], LaMnO [10], and $R_3Co_{11}B_4$ [11]. Several studies have been carried out on the R_6Fe_{23} compounds, e.g., magnetic properties, magnetostriction, electronic, and transport properties, as well as on crystal structure, lattice vibrations, and x-ray photoemission [12–19]. It is known that R_6Fe_{23} compounds crystallize in Th_6Mn_{23} type structure. Rare earth 4f-transition metals 3d intermetallic compounds show interesting magnetic properties. The two sublattice molecular field theory proved to be fairly suitable for calculating the magnetization of the compounds [12]. There are, however, few studies on the MCE of R_6Fe_{23}; therefore, our motivation to study in detail the magnetothermal properties and MCE (ΔS_m, ΔT_ad) in the R_6Fe_{23} system is justified. In addition, we calculated the relative cooling powers RCP(S) and RSP(T) as figures of merit. Investigating the order of the magnetic transition, via the temperature and field dependences of the magnetothermal and MCE properties, the universal curve, and the Arrott plots is also done.

2 Model and Analysis

By using the MFT, the exchange fields of rare earth elements and Fe sublattices can be expressed as follows [12, 20]:

$$H_R(T) = H + d\left[6n_{RR}M_R(T) + 23n_{RFe}M_{Fe}(T)\right] \quad (1)$$

$$H_{Fe}(T) = H + d\left[6n_{RFe}M_R(T) + 23n_{FeFe}M_{Fe}(T)\right] \quad (2)$$

The symbols in Eqs. (1) and (2) have their usual meaning [12]. The molecular field coefficients n_{RR}, n_{FeFe}, and n_{RFe} are dimensionless.

✉ Raghda Abu Elnasr
Raghda.ismp@gmail.com

[1] Department of Physics, Damietta University, New Damietta, Egypt

[2] Department of Physics, Helwan University, Helwan, Egypt

The magnetic moments of rare-earth $M_R(T)$ and iron $M_{Fe}(T)$ at temperature T.

$$M_R(T) = M_R(0)B_{J_R}[\frac{M_R(0)H_R(T)}{k_B T}] \tag{3}$$

$$M_{Fe}(T) = M_{Fe}(0)B_{J_{Fe}}\left[\frac{M_{Fe}(0)H_{Fe}(T)}{k_B T}\right] \tag{4}$$

$B_J(x)$ is the well-known Brillouin function and $x = \frac{M_J H}{k_B T}$

The total magnetic moment can be calculated from

$$M_{Total}(T) = 6M_R(T) \pm 23M_{Fe}(T) \tag{5}$$

From the following Maxwell relation, the magnetic entropy change is given by

$$\left(\frac{\partial S(T)}{\partial H}\right)_T = \left(\frac{\partial M(T)}{\partial T}\right)_H$$

$$\Delta S_M(T) = \int_{H_0}^{H_f} \frac{\partial M(T)}{\partial T} dH \tag{6}$$

The above integral could be cast into a summation by using the well-known trapezoidal rule [21].

A universal curve [22] is the relation between $\Delta S_m/\Delta S_m^{peak}$ vs. Θ.Where Θ is defined from the following:

$$\theta = (T - T_C)/(Tr - T_C),$$

where T_r is the reference temperature, it can be chosen such that [22]

$$\Delta S_m(Tr) = 0.7\Delta S_m^{peak} \tag{7}$$

The total heat capacity C_{tot} is calculated from the sum of the magnetic C_m, the electronic C_e, and the lattice C_l heat capacities [23, 24].

First, from the temperature-first derivative of the magnetic energy, we can calculate the magnetic contribution to heat capacity as the following equation:

$$U = -\frac{1}{2}[n_{RR}M_R^2(T) + n_{FeFe}M_{Fe}^2(T) + 2n_{RFe}M_R(T)M_{Fe}(T)] \tag{8}$$

$$C_M(T) = \frac{\partial U}{\partial T} \tag{9}$$

Second, the electronic heat capacity is calculated by [25]

$$C_e(T) = \gamma_e T = (\pi^2/3)N_a k^2 N(E_f)T \tag{10}$$

γ_e is the electronic heat capacity coefficient, and $N(E_f)$ is the density of states at Fermi energy.

Third, the lattice heat capacity is calculated as follows:

$$C_l(T) = 9NaK_B\left(\frac{T}{\theta_D}\right)^3 \int_0^{\theta_D/T} \frac{e^x x^4}{(e^x - 1)^2} dx \tag{11}$$

where Θ_D is Debye temperature and $x = \Theta_D / T$.

The adiabatic temperature change [23] is given by

$$\Delta T_{ad} = \int_{H_0}^{H_f} \frac{T}{C_{tot}(T,H)} \frac{\partial M(T)}{\partial T} dH \tag{12}$$

where C_{tot} is the total heat capacity.

The Arrott plots (M^2 vs. ΔS_m) and (H/M vs. M^2) are used to investigate the order of the phase transition from the sign of the plot's slopes. Namely, positive slopes indicate second-order phase transition, according to Arrot-Belov-Kouvel (ABK) [26, 27].

Ginsburg theory is expressed as follows [28]:

$$F = \frac{1}{2}A(T)M^2 + \frac{1}{4}B(T)M^4 + \frac{1}{6}C(T)M^6 - M.H \tag{13}$$

From the equilibrium condition at T_c, the magnetic equation of state is given by

$$\frac{H}{M} = A(T) + B(T)M^2 + \ldots \tag{14}$$

where A(T) and B(T) are Landau's coefficients.

The RCP [29] is considered as figure of merit for the magnetocaloric materials and is defined from magnetic entropy change as:

$$RCP(S) = \Delta S_{max}(T) * \delta T_{FWHM} \tag{15}$$

And also from the adiabatic temperature change,

$$RCP(T) = \Delta T_{max}(T) * \delta T_{FWHM} \tag{16}$$

3 Results and Discussion

3.1 Magnetization

Figure 1a–d exhibits the calculated magnetic moment of the two sublattices of rare earth R, Fe, and the total magnetic moment where R = Dy, Ho, Er, and Tm, respectively. Ferrimagnetic coupling is present in these compounds, with compensation points except for Tm_6Fe_{23}. We can show that the magnetic moment for Dy atom at 0 K is $M_{Dy}(0) = g_{Dy} J_{Dy} = (4/3) \times (15/2) = 10\ \mu_B$/atom. The magnetic moments

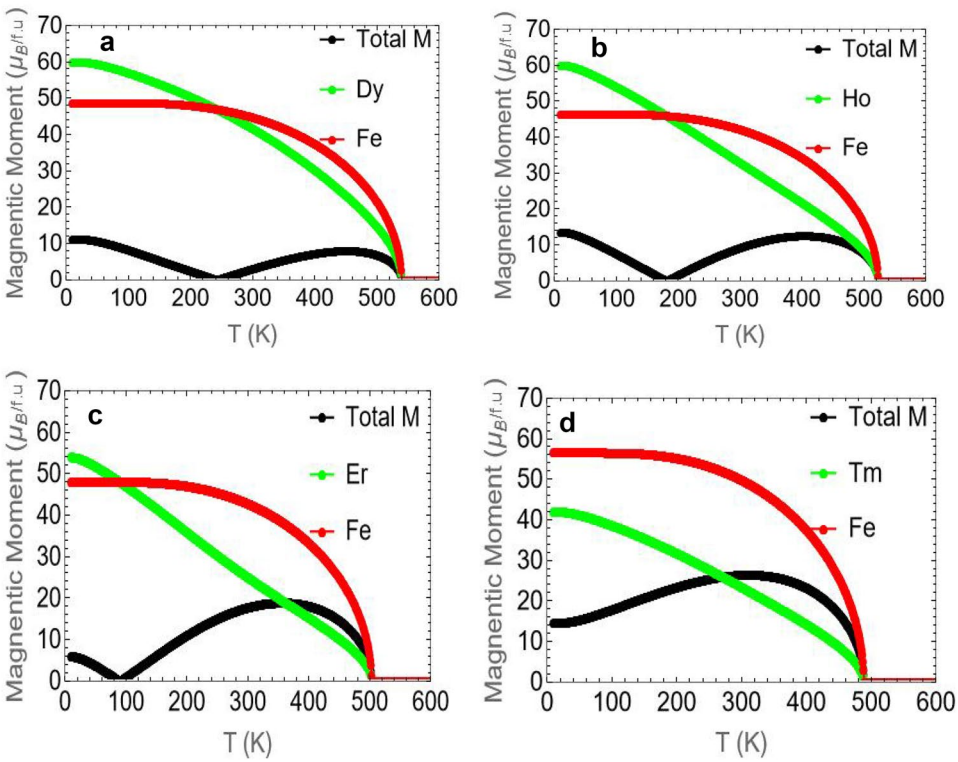

Fig. 1 Total and sublattice magnetizations vs. temperature in zero magnetic field for **a** Dy_6Fe_{23}, **b** Ho_6Fe_{23}, **c** Er_6Fe_{23}, and **d** Tm_6Fe_{23}

for R = Ho, Er, and Tm are calculated by Herbst and Croat [12]. As known, the magnetic moment for rare earth R is localized whereas that of the 3d-transition elements Fe in rare-earth intermetallic compounds. So, the magnetic moment of Fe sublattice is obtained from the experimental data of the total magnetic moment and the calculated magnetic moments of the rare earth R, for example, in Dy system $M_{Fe}(0) = 48.8/23 = 2.12\ \mu_B$/atom. Table 1 shows the experimental [12] and theoretical data of both the total magnetic moments and the Curie temperatures; for the R_6Fe_{23} system, also, the percentage difference between the experimentally determined moments and calculated magnetic moment at $T = 1$ K [12] is shown in Table 1. This difference is only $\leq 2.4\%$, and the difference in the T_c data is $\leq 2.86\%$. As shown, the mean field theory succeeded in studying the magnetization for R_6Fe_{23} and the rare earth intermetallic compounds such as $R_3Co_{11}B_4$ [11]. Magnetization calculations showed that, for example, both Dy_6Fe_{23} and $Dy_3Co_{11}B_4$ are ferrimagnetic compounds with the total magnetic moments 11.6 and 16.6 μ_B/f.u, respectively.

3.2 Total Heat Capacity

Figure 2 shows the field dependence of the magnetic heat capacity as function of temperature for Ho_6Fe_{23} at different magnetic fields up to 5 T. The maximum magnetic heat capacity decreases by increasing the applied field around Curie temperature, which is typical for compounds with second-order phase transition, for example, $Ho_3Co_{11}B_4$ [11] and $TmFe_2$ [7]. The electronic heat capacity is obtained from Eq. (10), and the coefficient γ_e is given from the materials project [30] as shown in Table 3. The lattice heat capacity is calculated from Debye temperature by Eq. (11). The Debye temperatures for most crystals are around room temperature.

Table 1 The calculated and experimental net magnetic moment, in zero field and 0 K, and the Curie temperatures for R_6Fe_{23} system

R	Magnetic moment (μ_B/f. u)		Percentage difference	T_c (K)		Percentage difference
	Cal	Exp		Cal	Exp	
Dy	11.6	11.89	2.4	540	529	2.07
Ho	13.5	13.79	2.1	523	509	2.75
Er	5.9	6.03	2.1	503	489	2.86
Tm	14.5	14.5	0	489	483	1.24

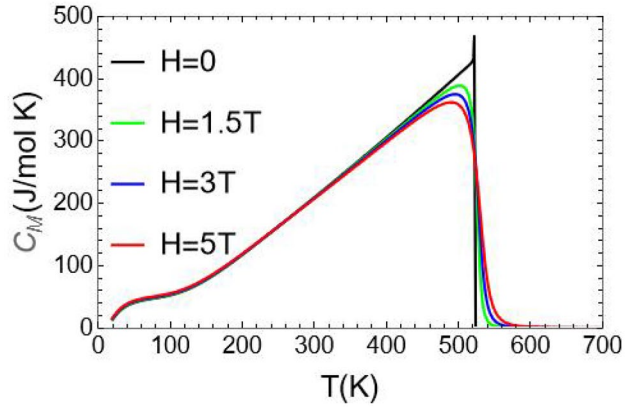

Fig. 2 Temperature dependence of magnetic specific heat for Ho_6Fe_{23} in external fields of 0, 1.5, 3, and 5 T

3.3 The Isothermal Entropy Change ($\triangle S_m$)

$\triangle S_m$ has been calculated using the Maxwell relation from Eq. (6) and also using the trapezoidal rule. Figure 3a–d shows ($\triangle S_m$ vs. T) at applied fields up to 5 T, for R = Dy, Ho, Er, and Tm, respectively. Both direct and inverse MCE, i.e., two peaks are present: the first peak at T_c and the second at a temperature below the compensation temperature. The data of magnetic entropy change ΔS_m using both Maxwell's relation and the trapezoidal rule showed agreement between the two methods, at low field changes, as shown in Table 2. For the sake of comparison with bench-mark materials and other R_6Fe_{23} compounds, we compare our results of ΔS_m, which is in the range of 3.9 to 9.8 J/mol K for a field change $\Delta H = 5$ T, with that of Gd metal, i.e., 1.48 J/mol K at $\Delta H = 5$ T as reported by Wang et al. [31], and also with Jemmali et al. [32], where ΔS_m of Er_6Fe_{23} is 3.64 J/mol K at $\Delta H = 1.4$ T.

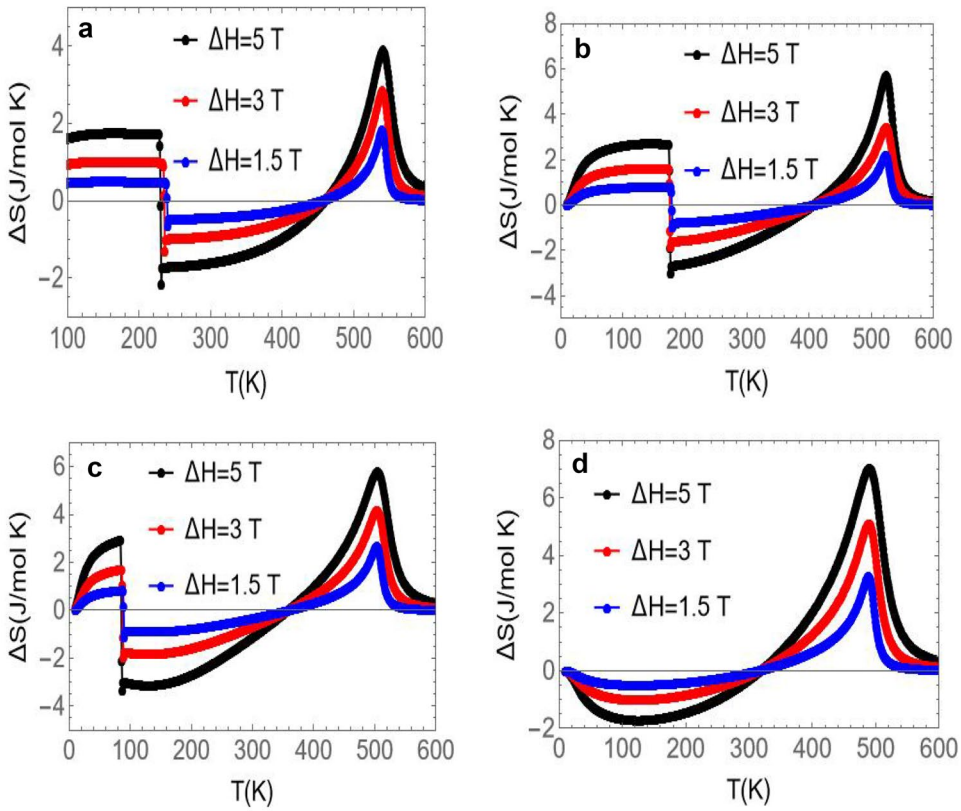

Fig. 3 Temperature dependence of the magnetic entropy change for **a** Dy_6Fe_{23}, **b** Ho_6Fe_{23}, **c** Er_6Fe_{23}, and **d** Tm_6Fe_{23}, for field changes of 1.5, 3, and 5 T

Table 2 The isothermal magnetic entropy change, for different magnetic field changes, in R_6Fe_{23} system using the trapezoidal and Maxwell methods

R	ΔS_m (J/K mol) Maxwell method			ΔS_m (J/ K mol) Trapezoidal method		
	$\Delta H = 5$ T	$\Delta H = 3$ T	$\Delta H = 1.5$ T	$\Delta H = 5$ T	$\Delta H = 3$ T	$\Delta H = 1.5$ T
Dy	3.9	2.8	1.8	4.9	3.3	1.9
Ho	4.7	3.4	2.2	6.2	4.2	2.3
Er	5.8	4.1	2.6	7.7	5.2	3.0
Tm	7.0	5.1	3.3	9.8	6.5	4.1

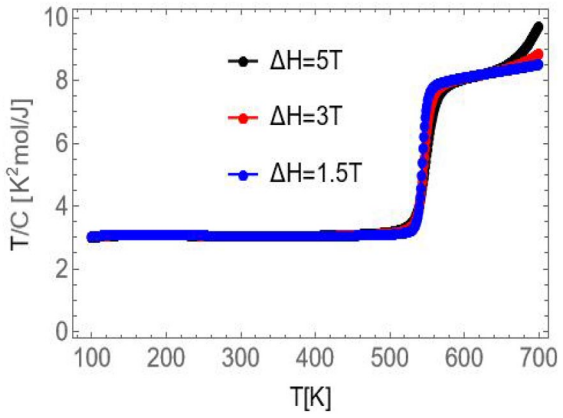

Fig. 4 The dependence of T/C on temperature in $H = 1.5$, 3, and 5 T for Dy_6Fe_{23}

3.4 Adiabatic Temperature Change (ΔT_{ad})

We report in this part ΔT_{ad}. Because of the weak dependence of the total heat capacity on the applied field, around Curie temperature for the R_6Fe_{23} compounds, as shown in Fig. 4 for example Dy_6Fe_{23} system, the term T/C is taken out of the integral in Eq. (12). Figure 5a–c shows the adiabatic temperature change ΔT_{ad} for R = Dy, Ho, and Tm using Eq. (12) for applied fields up to 5 T. The maximum value for ΔT is 15.17 K, as shown in Table 3 for applied field 5 T, and in the case of Tm_6Fe_{23}, the temperature is decreasing by a rate of 3.03 K/T.

3.5 Relative Cooling Power (RCP)

RCP is based on the isothermal process RCP(S), which is calculated by Eq. (15), for different field changes. The RCP(S) of Er_6Fe_{23} at a field of 1.4 T is 95.76 J/mol, as reported by Jemmali et al. [32], and also RCP(S) of Gd metal is 150.72 J/mol at field change 5 T as reported by Wang et al. [31]. Also, RCP is based on the adiabatic temperature change RCP(T) by Eq. (16). It has no physical meaning, but it is used for numerical comparison of other MC compounds. A large RCP(T) generally indicates a better magnetocaloric material, as shown in Table 5. The relative cooling power RCP(T) is in the range 449–1092 K^2 for a field change $\Delta H = 5$ T, which is compared with 967 K^2 of Gd at field 6 T, as reported by Gschneidner et al. [3]. The calculations show that the RCP(S) and RCP(T) increase with increasing the applied magnetic field, as shown in Tables 4 and 5.

Table 3 The adiabatic temperature change ΔT_{ad} (K), for different magnetic field changes, in R_6Fe_{23} system

R	DOS (1/eV)	γ_e ($_{mJ/mol\ K^2}$)	ΔT_{ad} (K)		
			$\Delta H = 5$ T	$\Delta H = 3$ T	$\Delta H = 1.5$ T
Dy	30	70.8	9.56	6.61	4.09
Ho	30	70.8	11.27	7.89	4.91
Tm	35	82.6	15.17	10.66	6.65

3.6 The Universal Curve and Arrott Plot

Figure 6 displays the universal curves (ΔS_m vs. Θ) for Dy_6Fe_{23} compound in applied fields of 1.5, 3, and 5 T. It can be clearly shown in Fig. 6 that the data of different applied fields collapse into a single universal curve, which shows the phase transition in the R_6Fe_{23} system is a second-order phase transition.

According to Arrot-Belov-Kouvel (ABK) [26, 27], the order of the phase transition involved the second-order SOPT or the first-order FOPT, from the sign of the plots

Table 4 Relative cooling power RCP(S) in J/mol for different field changes, in R_6Fe_{23} system

R	$\Delta H = 5$ T	$\Delta H = 3$ T	$\Delta H = 1.5$ T
Dy	148	95	45
Ho	256	153	70
Er	417	231	106
Tm	560	327	150

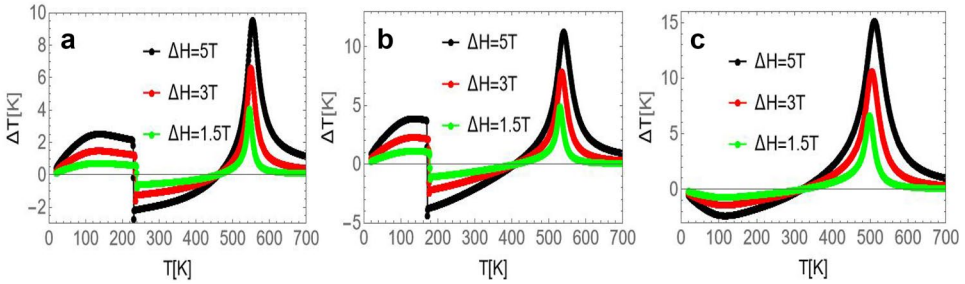

Fig. 5 Adiabatic temperature change vs. T for **a** Dy_6Fe_{23}, **b** Ho_6Fe_{23}, **c** Tm_6Fe_{23}, for field changes of 1.5, 3, and 5 T

Table 5 Relative cooling power RCP(T) in K^2 for different field changes, in R_6Fe_{23} system

R	$\Delta H = 5$ T	$\Delta H = 3$ T	$\Delta H = 1.5$ T
Dy	449	205	82
Ho	620	300	118
Tm	1092	554	220

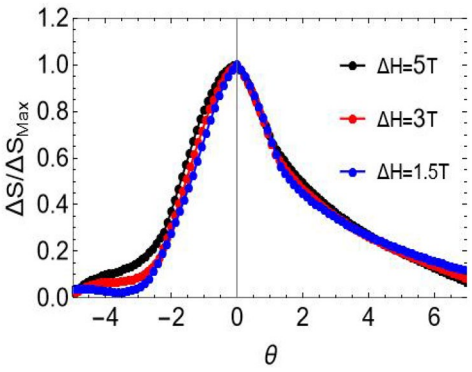

Fig. 6 Universal curves of the Dy_6Fe_{23} for field changes of 1.5, 3, and 5 T

slopes. Namely, positive slopes indicate SOPT, whereas negative slopes or s-shaped slopes indicate FOPT. Figure 7a, b shows (M^2) vs. (H/M) and ΔS_m vs. M^2 plots for the Dy_6Fe_{23} system; the positive slopes with a minimum around T_C indicate that the type of phase transition is SOPT.

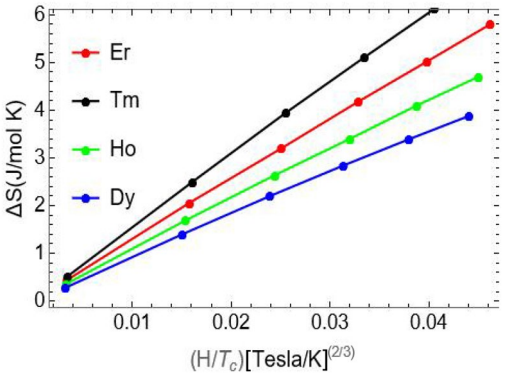

Fig. 8 ΔS_m vs. $(Tesla/K)^{2/3}$ for R_6Fe_{23} compounds in applied fields from 0.1 to 5 T

3.7 The Field Dependence of ΔS_m and the Critical Exponents

Figure 8 shows the ΔS_m vs. $(H/T_C)^{2/3}$ for R_6Fe_{23} compounds. According to the mean field theory, the relation ΔS_m vs. $(H/T_C)^{2/3}$ is a criterion for the existence of the SOPT [33, 34]. It would be instructive to evaluate some of the critical exponents [35–38] and compare them with those of the mean-field theory. We have calculated the parameters n, β, δ, and γ, where $n = 1 + (\beta - 1)/(\beta + \gamma)$ [37]. The parameter δ has been evaluated from the isothermal magnetization curve where $M \sim H^{1/\delta}$ [38].

The mean-field parameters are $\beta = 0.5$, $\gamma = 1$, and $\delta = 3$. Our calculation showed that β and γ are, at most, 8% and 16% off the mean-field values, respectively. The exponent δ is at most 30% off the mean-field value.

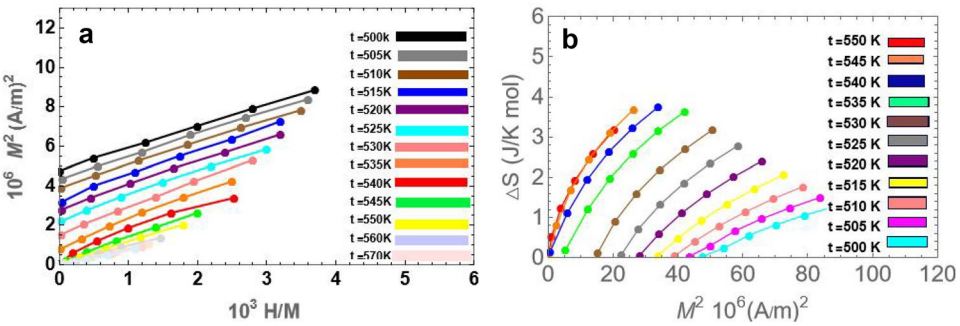

Fig. 7 **a** H/M vs. M^2 and **b** ΔS_m vs. M^2 for Dy_6Fe_{23} compound in applied fields of 0.1, 1, 2, 3,4, and 5 T. $T_c = 540$ K

4 Conclusion

We calculated the magnetothermal properties and magnetocaloric effect, ΔS_m and ΔT_{ad}, for R_6Fe_{23} compounds using the MFT. The magnetization calculation exhibited that the R_6Fe_{23} when R = Dy, Ho, Er, and Tm are ferrimagnetic compounds. The compensation point of the system is in the range of 86–230 K, and a Curie temperature is in the range of 489–540 K. For example, for R = Dy, the compensation point close to $T_{comp} = 240$ K and $T_c = 540$ K. The magnetic entropy change ΔS_m is calculated by Maxwell relation and by using the trapezoidal method. The highest ordinary MCE ΔS_m and ΔT_{ad} are 9.8 J/mol K and 15.17 K for R = Tm at applied field change 5 T. The RCP(S) is fairly comparable to those of Gd and Er_6Fe_{23}. The RCP(T) is in the range 449–1092 K^2 for a field change $\Delta H = 5$ T, which is comparable to that of bench-mark materials, e.g., Gd. The field and temperature dependencies of the magnetic moment, ΔS_m, ΔTa_d, the universal curves, and Arrott plots are investigated that the type of phase transition in the R_6Fe_{23} system is SOPT. The MFT is appropriate for studying the magnetic properties and MCE of the R_6Fe_{23} system.

Funding Open access funding provided by The Science, Technology & Innovation Funding Authority (STDF) in cooperation with The Egyptian Knowledge Bank (EKB).

Data Availability Authors agree to make the data available upon request.

Declarations

Conflict of Interest The authors declare no competing interests.

References

1. Andreenko, A.S., Nikitin, S.A., Tishin, A.M.: Magnetocaloric effects in rare-earth magnetic materials. Sov. Phys. USP. **32**, 649 (1989). https://doi.org/10.1070/PU1989v032n08ABEH002745
2. Brück, E.: Developments in magnetocaloric refrigeration. J. Phys. D: Appl. Phys. **38**, 381 (2005). https://doi.org/10.1088/0022-3727/38/23/R01
3. Gschneidner, K.A., Jr., Pecharsky, V.K.: Thirty years of near room temperature magnetic cooling. Int. J. Refrig. **31**, 945–961 (2008). https://doi.org/10.1016/j.ijrefrig.2008.01.004
4. Pecharsky, V.K., Gschneidner, K.A., Jr.: Magnetic refrigeration. John Willey & Sons (2002). https://doi.org/10.1002/0470845856.ch25
5. Tishin, A.M., Spichkin, Y.I.: Recent progress in magnetocaloric effect: mechanisms and potential applications. Int. J. Refrig. **37**, 223–229 (2014). https://doi.org/10.1016/j.ijrefrig.2013.09.012
6. Zhang, Y., Xu, X.: Machine learning the magnetocaloric effect in manganites from lattice parameters. Appl. Phys. A **126**, 341 (2020). https://doi.org/10.1007/s00339-020-03503-8
7. Nagy, A., Hammad, T., Yehia, S., Aly, S.H.: Thermomagnetic properties and magnetocaloric effect of $TmFe_2$ compound. J. Magn. Magn. Mater. **10**, 50 (2018). https://doi.org/10.1016/j.jmmm.2018.10.050
8. Elkhneny, R.M., Aly, S.H., Yehia, S., Khedr, D.M.: Magnetic properties and magnetocaloric effect of $R_2Fe_{14}B$ compounds with R = Y, Pr, Nd, Sm, Gd, Tb, Dy, Ho and high-magnetic field phase transitions in the compounds with R = Gd, Dy, Cryogenics. **127**, 103567 (2022). https://doi.org/10.1016/j.cryogenics.2022.103567
9. Elkenany, M.M., Aly, S.H., Yehia, S.: Magnetothermal properties and magnetocaloriceffect in transition metal-rich Gd-Co and Gd-Fe amorphous alloys. Cryogenics. **123**, (2022). https://doi.org/10.1016/j.cryogenics.2022.103439
10. Henchiri, C., Benali, A., Mnasri, T., Dhahri, E.: Modeling the magnetocaloric effect of $La_{0.8}$ MnO_3 by the mean-field theory. J. Supercond. Nov. Magn. **33**, 1143–1149 (2020). https://doi.org/10.1007/s10948-019-05316-0
11. Abu Elnasr, R., Aly, S.H., Yehia, S., Mohamed, F.Z.: Magnetothermal properties and magnetocaloric effect in $R_3Co_{11}B_4$. J Supercond Nov Magn (2022). https://doi.org/10.1007/s10948-022-06298-2
12. Herbst, J.F., Croat, J.J.: Magnetization of R_6Fe_{23} intermetallic compounds: molecular field theory analysis. J. Appl. Phys. **55**, 3023–3027 (1984). https://doi.org/10.1063/1.333293
13. Buschow, K.H.J., van der Goot, A.S.: Phase relations, crystal structures, and magnetic properties of erbium—iron compounds. Phys. Status Solidi. **35**, 515 (1969). https://doi.org/10.1002/pssb.19690350154
14. structural and magnetic properties of dysprosium-iron compounds: van der Goot, A. S. and. Buschow, K. H. J., The dysprosium-iron system. J. Less Com. Met. **21**, 151–157 (1970). https://doi.org/10.1016/0022-5088(70)90113-X
15. Croat, J.J.: Temperature dependence of the magnetostriction of polycrystalline Y_6Fe_{23}, Ho_6Fe_{23} and Er_6Fe_{23}. J. Magn. Magn. Mater. **15**, 597–598 (1980). https://doi.org/10.1016/0304-8853(80)90679-4
16. Gratz, E., Zuckermann, M.J.: Transport properties of rare earth intermetallic compounds (electrical resistivity, thermopower and thermal conductivity). J. Magn. Magn. Mater. **29**, 181–191 (1982). https://doi.org/10.1016/0304-8853(82)90238-4
17. Jemmali, M., Alleg, S., Dhahri, E., Bessais, L.: Effect of Al substitution on structural, magnetic, and magnetocaloric properties of $Er_6Fe_{23-}xAl_x$ (x = 0 and 3) intermetallic compounds. crystals. **7**, 156 (2017). https://doi.org/10.3390/cryst7060156
18. Smith, H.K., Rhyne, J.J., Hardman-Rhyne, K.A., Wallace, W.E.: Thermodynamic studies of hydrides of R_6Fe_{23} (R ≡ Y, Er, Ho, Lu) and R_6Mn_{23} (R ≡ Gd, Dy, Er, Ho). J. Less Comm. Meta. **130**, 421–429 (1987). https://doi.org/10.1016/0022-5088(87)90137-8
19. Robert, P.G., Wojciech, S.I., Zygmunt, Z.: Crystalline electric field effects in f-electron magnetism (1982) ISBN: 978–1–4684–8648–3. https://doi.org/10.1007/978-1-4684-8646-9
20. Khedr, D.M., Aly, S.H., Shabara, R.M., Yehia, S.: A molecular-field study on the magnetocaloric effect in Er_2Fe_{17}. J. Magn. Magn. Mater. **475**, 436–444 (2019). https://doi.org/10.1016/j.jmmm.2018.11.079

21. Tishin, A.M., Spichkin, Y.I.: The magnetocaloric effect and its applications. 1–3 (2003). ISBN: 0–7503–0922–9. https://doi.org/10.1016/S1369-7021(03)01134-9
22. Franco, V., Conde, A.: Scaling laws for the magnetocaloric effect in second order phase transitions. Int. J. Refrig. **33**(3), 465–473 (2010). https://doi.org/10.1016/j.ijrefrig.2009.12.019
23. de Oliveira, N.A., Von Ranke, P.J.: Theoretical aspects of the magnetocaloric effect. Phys. Rep. **489**, 89–159 (2010). https://doi.org/10.1016/j.physrep.2009.12.006
24. Debye, P.: On the theory of specific heats. Ann. Phys. **344**, 789–839 (1912). https://doi.org/10.1002/andp.19123441404
25. Kittel, C.: Introduction to solid state physics, 7 edition, John Wiley &Sons (1996). ISBN: 0–471–11181–3
26. Yeung, I., Roshko, R.M., Williams, G.: Arrott-plot criterion for ferromagnetism in disordered systems. Phys. Rev. B. **34**, 3456–3457 (1986). https://doi.org/10.1103/PhysRevB.34.3456
27. Banerjee, B.K.: On a generalized approach to first and second order magnetic transitions. Phys. Lett. **12**, 16–17 (1964)
28. Amaral, V.S., Amaral, J.S.: Magnetoelastic coupling influence on the magnetocaloric effect in ferromagnetic materials. J. Magn. Magn. Mater. **272**, 2104 (2004).https://doi.org/10.1016/j.jmmm.2003.12.870
29. Franco, V., Blazquez, J.S., Ingale, B., Conde, A.: The magnetocaloric effect and magnetic refrigeration near room temperature: materials and models. Annu. Rev. Mater. Res. **42**, 305–342 (2012). https://doi.org/10.1146/annurev-matsci-062910-100356
30. Lawrence, B.: materials project. (2020). https://doi.org/10.17188/1679719 https://doi.org/10.17188/1201803 https://doi.org/10.17188/1692983
31. Wang, G.F., Li, L.R., Zhao, Z.R., Yu, X.Q., Zhang, X.F.: Structural and magnetocaloric effect of $Ln_{0.67}Sr_{0.33}MnO_3$ (Ln=La, Pr and Nd) nanoparticles, J. Ceram. Int. **40**, 16449–16454 (2014). https://doi.org/10.1016/j.ceramint.2014.07.154
32. Jemmali, M., Alleg, S., Dhahri, E., Bessais, L.: Effect of Al substitution on structural, magnetic, and magnetocaloric properties of $Er_6Fe_{23-x}Al_x$ (x = 0 and 3) intermetallic compounds. Crystals **7**, 156 (2017). https://doi.org/10.3390/cryst7060156
33. Burzoa, E., Codescub, M.M., Kappeld, W., Helerarea, E.: Magnetic materials for technical applications. J. Optoelectron. Adv. M. **11**, 229–237 (2009)
34. Burrola, L.A., Andara, G., Rodriguez, C.R., Gomez, F.J., Saenz-Hernandez, R.J., Zubiate, M.E., Aquino, A.: Comparison of the order of magnetic phase transitions in several magnetocaloric materials using the rescaled universal curve, Banerjee and mean field theory criteria. J. Appl. Phys. **117**, 144 (2015). https://doi.org/10.1063/1.4918340
35. White, R.M., Geballe, T.H.: Long range order in solids, ch1. Academic press. ISBN: 0126077754 (1979)
36. George, A., Baker, J.R.: Quantitative theory of critical phenomena. ch.1. ISBN:978–0–12–075120–4 (1990). https://doi.org/10.1016/B978-0-12-075120-4.X5001-5
37. El Ouahbi, S., Yamkane, Z., Derkaoui, S., Lassri, H.: Magnetic properties and the critical exponents in terms of the magnetocaloric effect of amorphous $Fe_{40}Ni_{38}Mo_4B_{18}$ AlloY. J. Supercond. Nov. Magn. **34**, 1253 (2021). https://doi.org/10.1007/s10948-021-05832-y
38. Coey, J.M.D.: Magnetism and magnetic materials. Cambridge University Press (2009). https://doi.org/10.1017/CBO9780511845000